Journal of Mining and Environment (JME) Vol. 16, No. 6, 2025, 2087-2097

Shahrood University of Technology

Journal of Mining and Environment (JME)

Journal homepage: www.jme.shahroodut.ac.ir

Iranian Society of Mining Engineering (IRSME)

Evaluating the Impact of Mechanical Activation on the Microstructural Properties of Hematite Using Shape Parameter

Behzad Nemati Akhgar*

Mining Engineering Department, Engineering Faculty, Urmia University, Urmia, Iran

Article Info

Received 15 July 2025

Received in Revised form 5 August 2025

Accepted 20 September 2025

Published online 20 September 2025

DOI: 10.22044/jme.2025.16522.3231

Keywords

Hematite

X-ray diffraction

Shape parameter

Microstructure

Abstract

Researchers in various engineering fields are increasingly interested in evaluating the influence of the microstructural properties of minerals, such as hematite, on their reactivity. Hematite behaviour and microstructural changes during mechanical activation (MA) were investigated using the shape parameter. The laser diffraction analysis indicates the occurrence of agglomeration in the mechanically activated hematite after 60 min of MA. Based on the microstructural studies, the hematite crystallinity reduced to below 16% after 240 min of MA. Microstrain and crystallite size continuously changed during MA, leading to an increase in hematite leaching efficiency by sulfuric acid. The results revealed that the microstrain variation rate is higher than other microstructural parameters. The obtained shape parameter increased from about 0.31 in the initial hematite to 0.88 and 0.66 in the hematite mechanically activated for 60 and 240 min, respectively. The shape parameter study demonstrated that most mechanical energy is stored in the hematite lattice as microstrain after 240 minutes of MA. Considering the lower impact of microstrain on promoting hematite reactivity, shorter MA times could be preferred over prolonged MA, which would reduce costs and increase capacity.

1. Introduction

Hematite ore is an abundant rock-forming mineral in the Earth's crust and can be found in association with other valuable minerals [1-3]. Primary iron ores are magnetite and hematite, which are processed using various beneficiation methods such as magnetic separation, gravity separation, and flotation [4-7]. Since magnetite is a ferromagnetic mineral, it can be easily separated from other non-magnetic gangue minerals using low-intensity magnetic separators. However, the processing and separation of hematite is carried out using high-intensity magnetic separators due to its low magnetic susceptibility. Gravity methods can also be used to separate hematite if there is a sufficient difference in relative density between the valuable and gangue minerals [8-10]. Although numerous studies have been conducted on these methods and their limitations, particularly in cases where gangue minerals are locked within hematite grains, research focusing solely on physical methods is insufficient to address the challenges of efficient hematite processing fully. In addition, the hexagonal crystalline structure of hematite, its simple chemical composition (Fe_2O_3), its abundance, and its increasingly practical applications in various fields have made it an interesting topic for evaluation. The conversion of hematite to magnetic materials through roasting [11-14] and its dissolution to improve the quality of industrial minerals are the main applied issues related to hematite treatments [15-18]. Accordingly, investigating the thermal behaviour of hematite during roasting and examining the factors influencing its reactivity in dissolution processes becomes of significant importance. In this paper, we aim to address the gaps outlined in the following section by focusing on the latter aspect—specifically, the reactivity of hematite in the leaching process.

Corresponding author: b.n.akhgar@azad.ac.ir (B. Nemati Akhgar)

Due to the depletion of high-quality mineral reserves and various factors, such as improving industrial mineral properties by removing impurities like hematite, hematite hydrometallurgical processing has received significant attention. Furthermore, the most important practical issues concerning hematite are its removal from silicate and aluminium silicates such as clay, quartz, and kaolin [15-18]. Hematite's influence on gold leaching, the leaching mechanism of hematite, and its potential application in the preparation of advanced materials are other areas of investigation related to hematite [19-22]. In these studies [15-22], the role of pre-treatment methods such as mechanical activation (MA) and the associated structural changes in enhancing the processes mentioned above has received relatively little attention. Moreover, microstructural changes in hematite and other minerals during mechanochemical pretreatment methods, such as MA, were studied for process optimization. The obtained results proved that the reactivity of hematite has been enhanced after MA, and microstructural changes are responsible for that [19-22]. According to previous reports, the MA of sulphide and oxide minerals such as pyrite, hematite, and ilmenite can lower temperatures and increase reaction rates during their hydrometallurgical processes [23-29].

MA is a subset of mechanochemistry, along with mechanical alloying, mechanochemical activation, and mechanochemical reaction. In the case of MA, it has been performed by using high-energy ball milling to induce mechanical energy into mechanically activated minerals [23, 28, 30]. During MA, the induced energy is responsible for physical variations, physicochemical changes, and phase transformation in minerals, but their chemical composition remains unchanged. In addition to the alteration in bulk properties, such as particle size reduction and new surface formation during MA, the microstructural changes promote mineral reactivity and facilitate their participation in subsequent processes [23-30]. This way, MA simultaneously enhances both reaction efficiency and kinetics, even under moderate reaction conditions. In addition to the positive aspects of MA, investigating the microstructural parameters of mechanically activated minerals and their influence on mineral behaviour during subsequent processes, such as leaching, can provide valuable information for predicting mineral reactivity [23, 25]. Although structural changes during MA have been frequently investigated in previous studies, complementary parameters such as the shape factor have received less attention.

As mentioned, the microstructural changes and new surfaces created during high-energy grinding are the main factors that enhance the reactivity of mechanically activated minerals [23, 25-28, 30]. Therefore, the first question is which one of the surface changes or microstructural changes is the predominant factor affecting mineral reactivity. Recent studies have demonstrated that microstructural parameters enhance mineral reactivity after MA more significantly than the creation of new surfaces [25-27, 30]. Therefore, microstructural parameters like amorphization degree, crystallite size, and microstrain are essential to extract. The parameters can be extracted from XRD analysis of mechanically activated minerals through different approaches. Microstructural parameters are used to describe the properties of materials at the molecular and atomic levels in various ways. They can provide valuable information about atomic bond strength, atomic displacement, the number of reaction-ready atoms, and atom exchange during MA [25-27, 30]. The second question must be answered considering the different functions of these microstructure parameters: which is more important in promoting mineral reactivity? Previous findings have revealed that the crystallite size and microstrain variability differ in short and long periods of MA pyrite and chalcopyrite [25, 30]. The need for more sufficient data about hematite still hinders the comparison of microstructure parameters during MA. Therefore, the impact of microstrain and crystallite size on mechanically activated hematite, as well as their role in promoting reactivity, was examined during our investigation. The obtained result can provide practical and useful achievement, making proper decisions for hematite processing based on its microstructure properties and sensitivity.

Nowadays, using non-destructive and straightforward XRD analysis to predict the behaviour of materials and minerals during various processes is attracting growing attention [23-30]. The peak broadening and peak position shifts in XRD patterns of mechanically activated minerals result from microstructural changes, including a decrease in crystallite size and an increase in microstrain. Before extracting microstructural parameters from the broadened peaks, a fitting step should be performed on the XRD patterns using standard functions, such as Gaussian and Lorentzian, and their contributions [23, 26]. The shape parameter determines the contribution of the Gaussian (η=0) and Lorentzian (η=1) functions in

the fitting step of the diffraction patterns. A higher contribution of the Lorentzian function indicates the dominance of the crystallite size influence on peak broadening and hematite reactivity. Also, a higher contribution of the Gaussian function suggests the supremacy of microstrain [31]. This research aimed to evaluate the influence of MA on the promotion of hematite reactivity and determine the relationship between surface changes and microstructural parameters. The iron extraction, particle size, and microstructural parameters of hematite, including the amorphization degree, crystallite size, and microstrain, were measured, along with shape parameters. The results can provide a suitable opportunity to predict hematite behaviour during various processes.

2. Materials and Methods

2.1. Initial sample

The high-purity hematite sample was prepared by applying various concentration methods on a laboratory scale. A hematite concentrate sample obtained from the Golgohar Mining and Industrial company was manually ground to a particle size of – 75 μm. After that, low-intensity magnetic separation (for magnetite removal) and high-intensity magnetic separation (for quartz removal) were conducted on the hematite concentrate for its upgrading. For desulfurization, reverse flotation was performed in rougher and scavenger steps with potassium amyl xanthate (PAX) and MIBC at pH 7. Finally, the probable contaminations trapped between hematite particles (reverse flotation tailing) were removed by hand sorting and washing. XRD analysis was carried out on the sample to identify its constituent phases. It can be concluded from the obtained XRD pattern (Figure 1) that hematite (PDF No. 96-900-9783) is the primary component of the initial feed and is present as a single phase. According to the XRF analysis (XRF, PW2404 Philips), the sample contains approximately 97.1% hematite and minor impurities, including 1.3% SiO_2, 0.6% Al_2O_3, 0.3% CaO, 0.2% MgO, and 0.1% MnO.

2.2. Mechanical Activation and Leaching Tests

Operating variables of leaching tests and the MA process were selected based on preliminary tests and prior literature to ensure moderate and representative conditions for these processes. A laboratory planetary ball mill (NARYA–MPM2*250H, Amin Asia Fanavar Pars, Iran) was employed to grind hematite with a rotation speed of 400 rpm for 60 and 240 minutes under an air atmosphere. During the MA step, 10 Stainless steel balls with a diameter of 20 mm were used in a ball-to-powder weight ratio of 20. The amount of hematite loaded into each vial for MA was approximately 15 g. After MA, the samples were packaged under standard conditions and stored in a refrigerator. The leaching experiments were conducted on a 10 g sample in a 500 mL beaker using 300 mL 1 M sulfuric acid at 25 °C for 5 hours with mechanical agitation at 400 rpm. After the completion of each leaching experiment, the leach liquor was filtered, and approximately 10 mL of the filtrate was subjected to atomic absorption spectroscopy for iron concentration measurement. Atomic absorption spectroscopy (Varian 280FS, Australia) was used to measure the iron extraction at the end of the leaching process for initial hematite and mechanically activated samples. The leaching experiments were conducted twice, and the mean values were used for analysis.

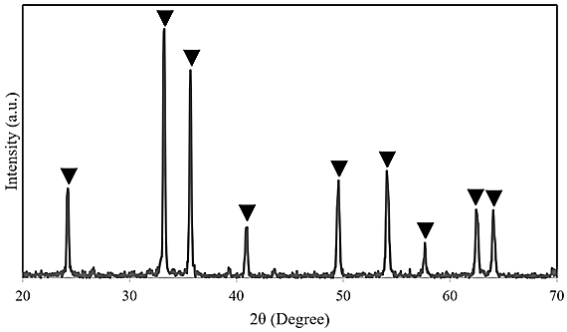

Figure 1. XRD pattern of initial hematite sample (hematite ▼)

2.3. Characterization

XRD analyses were performed using a Bruker Axs D8 advanced instrument (Germany) by applying Cu Kα radiation (λ = 1.5406 Å) at 50 kV and 250 mA in the two theta ranges of 20°–70°. These patterns were employed to identify the constituent phases of initial hematite and the powders obtained from MA. Microstructural parameters, including the amorphization degree, crystallite size, and microstrain, were determined using the Rietveld method. The X'pert high score plus software was used for phase identification and microstructural study through the Rietveld refinement method. Measuring shape parameters was conducted through profile fitting steps with the X'pert high score software.

The sensitivity of primary XRD characterization depends on the accuracy of input data extraction, such as the peak position, maximum intensity of diffraction peaks, full-width at half maximum (FWHM), and the shape

parameter (mixing factor- η) of fitting functions. First, the $K\alpha_2$ component and background were subtracted from the obtained XRD patterns, and the nine most intense peaks were selected for profile fitting. The combination of Cauchy and Gaussian functions (Pseudo-Voigt function) was applied in the profile fitting step. A particle size analyser instrument (ANALYSETTE 22 Nano Tec plus, FRITSCH, Germany) was utilized to measure the mean particle size and granulometric-specific surface area. A schematic roadmap of the approach followed to compare the influence of microstructural properties on mechanically activated hematite is depicted in Figure 2.

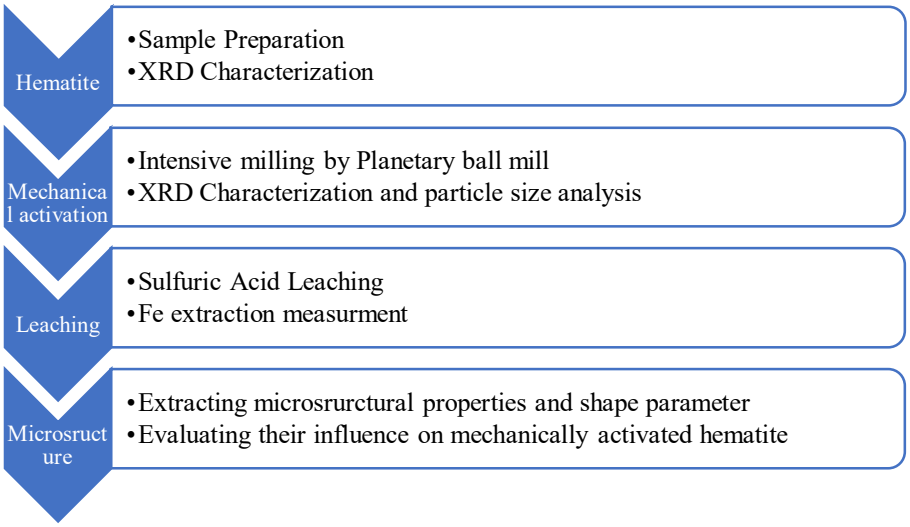

Figure 2. A schematic roadmap used in this study for evaluating microstructural changes of mechanically activated hematite

3. Results and Discussion

3.1. Primary XRD Characterization

The initial step was to identify the impact of MA on the constituent phase transformation of hematite. The XRD patterns of hematite after 60 and 240 min MA are depicted in Figure 3. The mechanical energy induced during MA was insufficient to initiate a mechanochemical reaction, and there was no new phase formed in addition to hematite, as previously reported [23]. Despite the severe milling conditions used under an air atmosphere, phase transformation was not observed in hematite, like pyrite, chalcopyrite, and ilmenite [23, 26-30]. The prolonged MA time resulted in significant microstructural changes in the hexagonal structure of hematite, as evidenced by the broadening and weakening of XRD reflection peaks. Using the Rietveld method, the microstructure parameters of hematite during MA will be extracted, and their variability will be discussed.

The highest hematite peak at 33.2 degrees was selected for a deeper examination before studying the microstructural changes (Figure 4). As evident in Figure 4, the intensity of the peaks decreases, and they broaden during hematite MA. Also, the position corresponding to the highest hematite peak shifted towards higher diffraction peak positions of 33.29 and 33.31 degrees after 60 and 240 min of MA. Due to the peak position shift, the interplanar spacing (d) has to be decreased during MA, according to the Bragg equation (Eq. 1).

$$n\lambda = 2d\sin\theta \quad (1)$$

, where d is the interplanar spacing and n is the order of reflection (n = 1, 2, 3, and…).

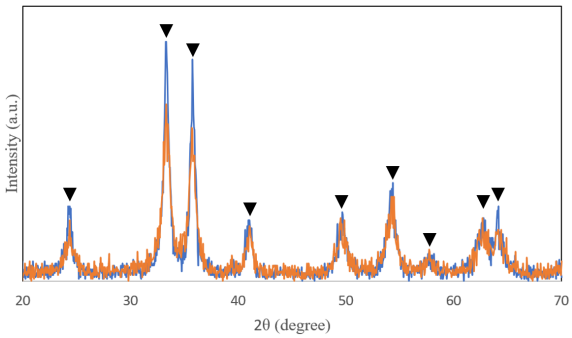

Figure 3. XRD patterns of mechanically activated hematite (hematite ▼, Blue: 60 min MA, Orange: 240 min MA)

The lattice constant as a function of temperature, phase transformation, and composition is a crucial piece of information for

modelling microstructure evolution [32]. Interplanar spacing (d) and lattice parameters vary during the MA process due to elements entering and leaving the hematite structure [26]. The result confirmed that the interplanar spacing (d) has decreased with prolonged milling (Figure 5). The atoms that have left the hematite structure during MA could be the reason for the lower interplanar spacing (d). Furthermore, the contraction of the hematite structure due to the intensive impact of milling media during MA might be another reason for the decrease in interplanar spacing (d).

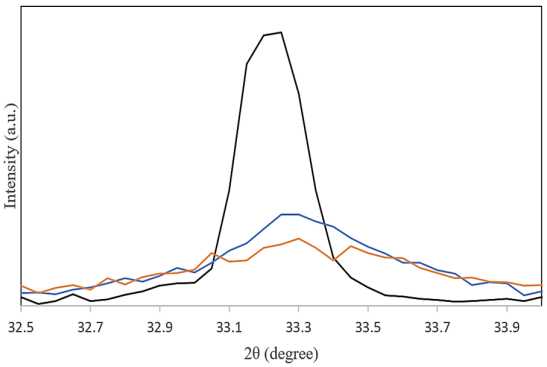

Figure 4. Peak shift of the strongest peak of hematite after MA (Black: hematite, Blue: 60 min MA, Orange: 240 min MA)

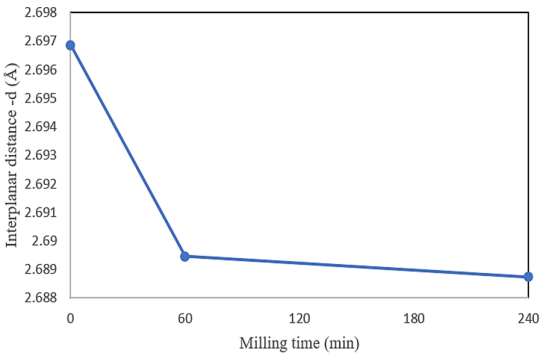

Figure 5. Variation of hematite interplanar distance (d) during MA

3.2. Microstructural properties

Table 1 summarizes the changes in peak intensity, full width at half maximum (FWHM), and other microstructural parameters. While prior studies indicate that structural changes during MA are typically minor at short time intervals [26], incorporating intermediate points (e.g., 120 min) could provide further insight into microstructure and surface parameters evolution, and is recommended for future investigations. The results proved that peak intensity and FWHM changes were more pronounced during the initial 60-minute MA than during the next 180-minute MA. The intensive variation during the first 60 min of MA indicates that microstructural changes mostly happened during the short period of MA. Microstructural changes can be quantified by measuring microstructural parameters, including amorphization degree, crystallite size, and microstrain. The evaluation of microstructural changes in hematite during MA begins with measuring the amorphization degree, as previously cited [33]. According to the results, the amorphization degree increases with milling time (Table 1). The increase in amorphization degree results from the weakening of interatomic bonds [25, 34], which leads to an increase in the reactivity of hematite. The microstrain is the following parameter that reflects the displacement of atoms in the hematite lattice [35-36]. The materials' reactivity is also promoted as the microstrain rises during intensive milling [24-27]. It was found that hematite microstrain extended with MA, indicating that hematite reactivity improved. The following microstructure parameter was the crystallite size, which is inversely proportional to the number of atoms ready to react in a material [37]. As shown in Table 1, MA reduces the crystallite size of hematite, thereby promoting the reactivity of mechanically activated hematite. The reduction in crystallite size of hematite during MA is consistent with previous studies on hematite and other materials such as ilmenite, pyrite, and chalcopyrite that have undergone MA [23, 25-30]. Consequently, hematite reactivity must elevate when the crystallite size decreases and the microstrain and amorphization degree increase.

Table 1. Variation of FWHM, main peak intensity, and microstructural properties of hematite during MA

MA (min)	FWHM (degree)	Peak intensity (cts)	Microstrain (%)	crystallite size (nm)	amorphization degree (%)
0	0.1692	313	0.023	71	0
60	0.8294	76	0.074	13	78
240	0.5692	50	0.16	9.2	84

3.3. Leaching tests and evaluating the MA Influences on hematite

The study continued to answer how these microstructure parameters affect the reactivity of mechanically activated hematite. This section compares the effects of structural and surface changes and determines the dominant parameter in promoting hematite reactivity. To attain this goal, hematite and mechanically activated powders were subjected to leaching experiments. In leaching experiments with one molar sulfuric acid at ambient temperature, the iron extraction from mechanically activated hematite increased compared to the initial hematite leached (Figure 6). Thus, the results of the leaching experiment confirmed that MA promotes the reactivity of hematite. After 60 and 240 min, iron extraction increased by 3.8 and 4.3 times in comparison with Fe extraction from initial hematite, respectively. It's worth mentioning that MA induces microstructural changes and decreases particle size, increasing the surface area of hematite. Figure 7 depicts how hematite's surface area and particle size change during MA. Initially, the hematite concentrate exhibited a particle size of 3.7 µm and a specific surface area of 2.6 m²/g. After 60 minutes of MA, the particle size decreased to 1.7 µm, accompanied by a doubling of the specific surface area to 5.2 m²/g. However, prolonging the MA time to 240 minutes resulted in a slight increase in particle size to 1.8 µm and a marginal decrease in surface area to 4.8 m²/g. As indicated, the particle size increases after 60 minutes of MA, marking the beginning point for particle agglomeration during hematite MA. This trend suggests the onset of agglomeration—a common phenomenon in prolonged high-energy milling processes. As particles become finer and their surface energy increases, they tend to re-aggregate or form loosely bonded clusters to minimize instability [23, 26, 28]. To mitigate this, wet milling or dispersant additives could be considered in future studies.

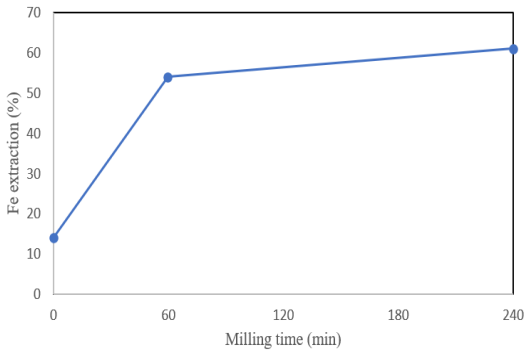

Figure 6. Leaching efficiency of initial hematite, 60 and 240 min mechanically activated hematite

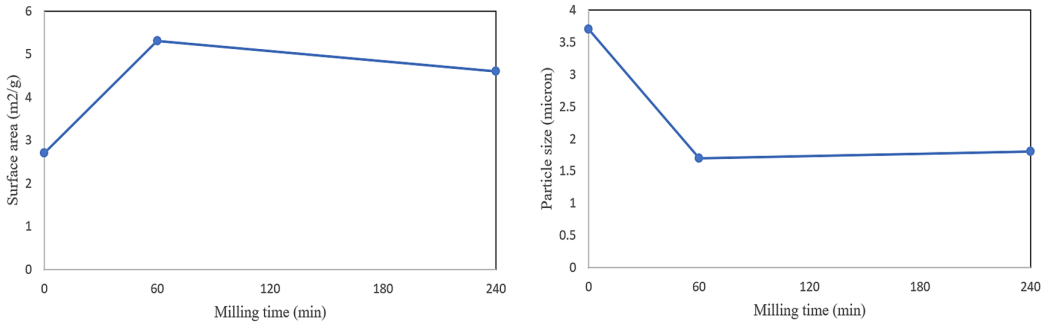

Figure 7. Granular surface area (Left) and particle size (Right) variation of hematite during MA

The comparison of surface and microstructural parameters was performed by investigating the effect of the surface area parameter on iron extraction and hematite reactivity. The variation of iron extraction versus surface area is depicted in Figure 8. The results uncovered that the Fe extraction increased from 14±1.6% in initial hematite with 2.7 m^2/g surface area to 54±2.3% after 60 min MA with 5.4 m^2/g surface area and 61±3.2% for 240 min mechanically activated hematite with 4.6 m^2/g surface area. Despite the decreased surface area of the 240 min mechanically activated hematite (star mark in Figure 8), the iron extraction has still increased. As a result, it can be concluded that the increase in surface area is not the primary factor contributing to the promotion of hematite reactivity. Consequently, the microstructure parameters such as amorphization degree or crystallinity, crystallite size, and microstructure are effective factors in enhancing the reactivity of hematite. In the following, an attempt was made to determine the importance of each microstructure parameter in hematite reactivity and its behavior prediction.

The comparison of microstructural parameters, including crystallinity, microstrain, and crystallite

size, involved evaluating their variability during hematite MA (Figure 9). The variability of microstructure parameters was obtained by calculating the variation ratio between mechanically activated hematite at 60 and 240 min and nonactivated hematite. To address the issue of zero amorphization degree in the non-activated samples, the crystallinity measure was used in the calculation instead of the amorphization degree. The crystallinity was obtained by subtracting the amorphization degree from 100. The microstrain variation ratio increased dramatically by 596% after 240 min of MA, indicating a substantial accumulation of lattice defects and internal stresses due to intense mechanical impacts. Concurrently, the crystallite size variation ratio decreased by 87% after 240 min of MA, reflecting extensive particle refinement and fragmentation at the nanoscale, which is characteristic of prolonged high-energy milling. Furthermore, the crystallinity variation ratio decreased by 84% after 240 min of MA, corresponding to a significant increase in amorphization. This pronounced loss of long-range atomic order suggests severe structural disordering and partial transformation of the crystalline phase toward an amorphous or nanocrystalline state. The findings indicated that the variation intensity of microstructural parameters can be ordered by microstrain, crystallite size, and crystallinity (amorphization degree). According to the leaching results, the iron extraction slightly increases in the 240 min mechanically activated hematite compared to the 60 min mechanically activated hematite (Figure 6). While Figure 9 shows the extent of variation in each parameter, the effectiveness in enhancing reactivity (assessed via leaching tests) was highest for crystallinity reduction. This comparison helps underline that not all parameter variations contribute equally to reactivity, and such insight is critical for process optimization. Therefore, the effectiveness order of microstructure parameters on hematite reactivity is crystallinity (amorphization degree), crystallite size, and microstrain, contrary to the order mentioned earlier based on the variation ratios. Hence, hematite reactivity is influenced the most by the amorphization degree among the microstructural parameters, while the microstrain has the least influence.

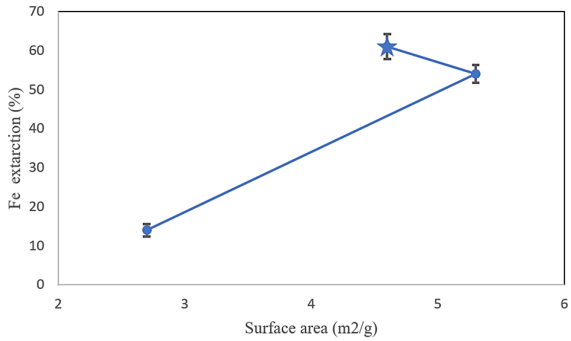

Figure 8. Variation of leaching efficiency with hematite surface area

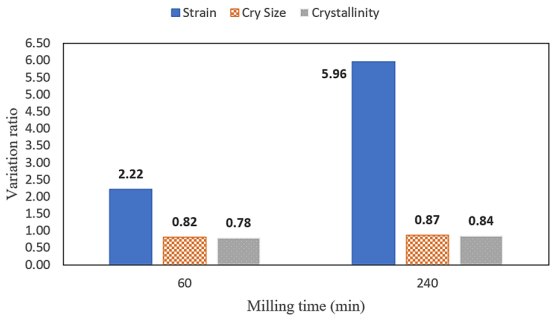

Figure 9. Variation ratios of microstructural parameters of mechanically activated hematite to nonactivated hematite

3.4. Shape Parameter (η)

The shape parameter (η) is influenced by both crystallite size and microstrain, but cannot fully account for other defect types such as dislocations, stacking faults, or twins. The parameter provides an approximate trend for microstrain and crystallite size variations during MA. The shape parameter study reveals that it increases from 0.31 in the initial hematite to 0.88 in the hematite after 60 min of MA (Figure 10). After 240 min of MA, the shape parameter was measured at a value of 0.66. Therefore, it is found that in initial hematite, the broadening of diffraction peaks is affected more by intrinsic microstrain. Due to the geological conditions and sample preparation, the intrinsic microstrain is the dominant factor responsible for the peak broadening in the XRD patterns of initial hematite. The results are consistent with the shape parameter of initial pyrite found in previous studies on pyrite behaviour during MA [26]. The shape parameter demonstrated that after 60 minutes of MA, the effect of crystallite size makes the most significant contribution to peak broadening. The shape parameter decreased from 0.88 in mechanically activated hematite after 60 min to 0.66 in the sample after 240 min of MA.

Consequently, the rate of reduction in crystallite size decreases with extended MA, and as milling continues, an increasing amount of mechanical energy is devoted to altering the microstrain. Therefore, most of the mechanical energy contributes to breaking particles and reducing crystallite size during the initial phase of MA (60 min of MA). As milling progresses, the opportunity for further crystallite size reduction and particle size decrease diminishes due to structural limits and the onset of agglomeration. Consequently, additional mechanical energy begins to accumulate as lattice distortion and defect formation, which manifests as increased microstrain, as reported before [23, 28]. The results obtained from the analysis of shape factor variations are consistent with the findings from the study of the variation ratio parameter (Figure 9), where the extent of microstrain change increases significantly from 2.22 in the sample with 60 min MA to 5.96 in the 240 min sample. In contrast, the change in crystallite size remains minimal, with only a 0.05 unit reduction (from 0.82 to 0.87), further confirming that prolonged MA predominantly enhances microstructural distortions rather than further refining crystallite size.

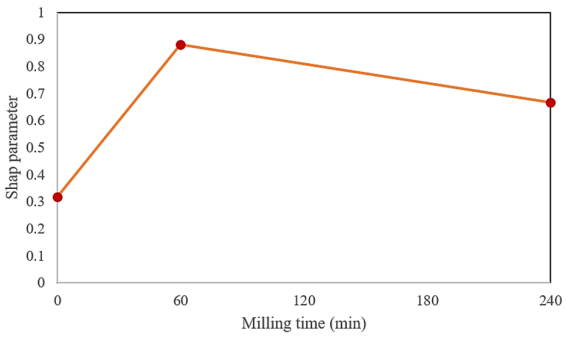

Figure 10. Shape parameter variation during hematite MA

According to the results, the MA significantly changes the shape parameter obtained from the profile-fitting step of XRD patterns. The contribution of crystallite size and microstrain to peak broadening, microstructural changes, and promotion of hematite reactivity differs during hematite MA, depending on the shape parameter. The results indicate that the decreasing rate of crystallite size reduces, and the increasing rate of microstrain rises with MA time. Therefore, extending the MA has the most significant impact on microstrain, which is the microstructural parameter with the lowest effect on hematite reactivity compared to other microstructural parameters. Thus, a prolonged MA time resulted in a more significant loss of stored mechanical energy in mechanically activated hematite due to the higher microstrain variation rate. For this reason, short-term MA should be preferred over long-term MA, as it minimizes MA duration and costs, enhances energy efficiency, and boosts the operational capacity of associated processes.

4. Conclusion

The most significant achievement was identifying crystallinity (amorphization degree) as the most influential factor for increasing hematite reactivity. Other main findings of this study can be summarized as follows:

- Mechanical activation (MA) of hematite enhances its reactivity toward sulfuric acid leaching without altering its crystal phase.
- XRD analysis showed that MA leads to decreased crystallite size, increased microstrain, and increased amorphization, all contributing to improved leachability.
- The Fe extraction increased by 3.8-fold and 4.3-fold after 60 and 240 minutes of MA, respectively.
- The effectiveness of MA in improving reactivity is more strongly linked to microstructural changes than to surface area increase or particle size reduction.
- Among the microstructural parameters, crystallinity has the highest impact on reactivity, followed by crystallite size and microstrain.
- The shape parameter (η) provided insights into how mechanical energy is stored and transformed during MA: shorter milling times favour crystallite size reduction, while prolonged MA mainly increases microstrain.
- Prolonged MA may lead to less efficient use of mechanical energy due to the lower reactivity effect of microstrain, suggesting that shorter milling durations may be preferable in industrial practice.

Future studies could investigate intermediate MA times (e.g., 90 or 120 minutes) better to understand the transition in microstructural changes of hematite. Applying statistical optimization methods such as DOE is recommended for a more accurate hematite MA process design. Additionally, using alternative milling media and advanced techniques like TEM or Raman spectroscopy can provide deeper insight into the defect structures of hematite during MA.

Declaration of interests

The authors declare that they have no conflict of interest.

References

[1]. Wills, B.A. (1985). Mineral processing technology, 3rd ed., Pergamon Press, Oxford, 521 P.

[2]. Clout, J.M.F., & Manuel, J.R. (2015). Mineralogical, chemical and physical characterization of iron ore. In: Lu, L. (Ed.), Iron Ore, Woodhead Publishing, Oxford, pp. 45–84.

[3]. Kiptarus, J.J., Muumbo, A.M., Makokha, A.B., & Kimutai, S.K. (2015). Characterization of selected mineral ores in the eastern zone of Kenya: case study of Mwingi North Constituency in Kitui County. *International Journal of Mining Engineering and Mineral Processing,* 4, 8–17.

[4]. Akhgar, B.N., Kheiri, S., Faridazad, M., Chehreghani, S., & Bahrami, A. (2024). Modification of mineral processing circuit in Arjin mine through a mineralogical study: magnetic separation and reverse flotation. *Iranian Journal of Earth Science,* 16, 1–9.

[5]. Saravari, A., Sam, A., & Shayanfar, S. (2021). Desulfurization of iron ore concentrate using a combination of magnetic separation and reverse flotation. *Journal of Chemical Technology and Metallurgy,* 56: 1102–1110.

[6]. Yu, J., Ge, Y. and Cai, X. (2016). The desulfurization of magnetite ore by flotation with a mixture of xanthate and dixanthogen. *Minerals,* 6, 70.

[7]. Bai, S., Li, J., Bi, Y., Yuan, J., Wen, S., & Ding, Z. (2023). Adsorption of sodium oleate at the microfine hematite/aqueous solution interface and its consequences for flotation. *International Journal of Mining Science and Technology,* 33, 105–113.

[8]. Song, S., Zhang, G., Luo, Z., & Lv, B. (2019). Development of a fluidized dry magnetic separator and its separation performance tests. *Mineral Processing and Extractive Metallurgy Review,* 40, 307–313.

[9]. Mackay, D.A.R., Simandl, G.J., Luck, P., Grcic, B., Li, C., Redfearn, M., & Gravel, J. (2015). Concentration of carbonatite indicator minerals using a Wilfley gravity shaking table: a case history from the Aley carbonatite. *Geological Fieldwork 2014, British Columbia Geological Survey Paper*, pp. 189.

[10]. Vinhal, J.T., Costa, R.H., Junior, A.B.B., Espinosa, D.C.R., & Tenório, J.A.S. (2020). Gravity separation of zinc mine tailing using Wilfley shaking table to concentrate hematite. In: *Energy Technology 2020: Recycling, Carbon Dioxide Management, and Other Technologies*, Springer International Publishing.

[11]. Prusti, P., Rath, S.S., Dash, N., Meikap, B.C., & Biswal, S.K. (2021). Pelletization of hematite and synthesized magnetite concentrate from a banded hematite quartzite ore: A comparison study. *Advanced Powder Technology,* 32, 3735–3745.

[12]. Haghi, S.M.A., Zabett, A., & Mirjalili, M. (2021). The mechanism of the reduction of hematite-magnetite concentrate by graphite-calcium carbonate mixture in Hoganas process. *Journal of Metallurgical and. Materials Engineering,* 32, 45–56.

[13]. Liang, Z., Peng, X., Huang, Z., Chen, J., Li, J., Yi, L., & Huang, B. (2023). Non-isothermal reduction kinetics of low-grade iron ore–coal mini-pellet in a low-temperature rotary kiln process. *Materials Today Communications,* 35, 105607.

[14]. Yu, J., Sun, H., Sun, X., Guo, Y., Zhang, W., & Li, Y. (2025). Kinetic study on low-temperature reduction of hematite in a microfluidized bed: Effect of pore characteristics on reaction rate. *Materials Today Communications,* 46, 112886.

[15]. Huang, H., Li, J., Li, X., & Zhan, Z. (2013). Iron removal from extremely fine quartz and its kinetics. *Separation and Purification Technology,* 108, 45–50.

[16]. Lee, S.O., Tran, T., Jung, B.H., Kim, S.J., & Kim, M.J. (2007). Dissolution of iron oxide using oxalic acid. *Hydrometallurgy,* 87, 91.

[17]. Martínez-Luévanos, A., Rodríguez-Delgado, M.G., Uribe-Salas, A., Carrillo-Pedroza, F.R., & Osuna-Alarcón, J.G. (2011). Leaching kinetics of iron from low grade kaolin by oxalic acid solutions. *Applied Clay Science,* 51, 473–477.

[18]. Tuncuk, A., & Akcil, A. (2016). Iron removal in production of purified quartz by hydrometallurgical process. *International Journal of Mineral Processing,* 153, 44–50.

[19]. Feng, D., & van Deventer, J.S.J. (2007). Effect of hematite on thiosulphate leaching of gold. *International Journal of Mineral Processing,* 82, 138–147.

[20]. Salmimies, R., Mannila, M., Kallas, J., & Häkkinen, A. (2012). Acidic dissolution of hematite: Kinetic and thermodynamic investigations with oxalic acid. *International Journal of Mineral Processing,* 110–111, 121–125.

[21]. Carmignano, O.R., Vieira, S.S., Teixeira, A.P.C., Lameiras, F.S., Brandão, P.R.G., & Lago, R.M. (2021). Iron ore tailings: Characterization and applications. *Journal of the Brazilian Chemical Society,* 32, 1895–1911.

[22]. Nyarige, J.S., Krüger, T.P.J., & Diale, M. (2020). Influence of precursor concentration and deposition temperature on the photoactivity of hematite electrodes for water splitting. *Materials Today Communications,* 25, 101459.

[23]. Pourghahramani, P., & Forssberg, E. (2006). Microstructure characterization of mechanically activated hematite using XRD line broadening.

International Journal of Mineral Processing, 79, 106–119.

[24]. Ermolovich, E.A., & Ermolovich, O.V. (2016). Effects of mechanical activation on the structural changes and microstructural characteristics of the components of ferruginous quartzite beneficiation tailings. *International Journal of Mining Science and Technology,* 26, 1043–1049.

[25]. Akhgar, B.N., & Pourghahramani, P. (2015). Impact of mechanical activation and mechanochemical activation on natural pyrite dissolution. *Hydrometallurgy,* 153, 83–87.

[26]. Pourghahramani, P., & Akhgar, B.N. (2006). Characterization of structural changes of mechanically activated natural pyrite using XRD line profile analysis. *International Journal of Mineral Processing,* 134, 23–28.

[27]. Pourghahramani, P., & Akhgar, B.N. (2015). Influence of mechanical activation on the reactivity of natural pyrite in lead (II) removal from aqueous solutions. *Journal of Industrial and Engineering Chemistry,* 25, 131–137.

[28]. Balaz, P. (2003). Mechanical activation in hydrometallurgy. *International Journal of Mineral Processing,* 72, 341–354.

[29]. Akhgar, B.N., Pazouki, M., Ranjbar, M., Hosseinnia, A., & Salarian, R. (2012). Application of Taguchi method for optimization of synthetic rutile nanopowder preparation from ilmenite concentrate. *Chemical Engineering Research and Design,* 90, 220–228.

[30]. Akhgar, B.N., Kavanlouei, M., Farhoudi, S., & Rohzad, M.H. (2024). Impact of mechanical activation and mechanochemical activation on microstructural changes, leaching rate and leachability of natural chalcopyrite. *Mineral Engineering,* 217, 108962.

[31]. Clearfield, A., Riebenspies, J.H., & Bhuvanesh, N. (2009). *Principle and Application of Powder Diffraction*, 1st ed., Wiley-Blackwell, Hoboken, 426 P.

[32]. Chen, L.Q., & Gu, Y. (2014). Computational Metallurgy. In: Laughlin, D.E. and Hono, K. (Eds.), *Physical Metallurgy*, 5th ed., Elsevier, Oxford, pp. 2807–2835.

[33]. Norrish, K. (1962). Quantitative analysis by X-ray diffraction. *Clay Minerals,* 5(28), 98–109.

[34]. Tahmasebi, R., Shamanian, M., Abbasi, M.H., & Panjepour, M. (2009). Effect of iron on mechanical activation and structural evolution of hematite-graphite mixture. *Journal of Alloys and Compounds,* 472, 334–342.

[35]. Cullity, B.D., & Stock, S.R. (2009). *Elements of X-ray Diffraction*, 3rd ed., Prentice Hall, New Jersey, 664 P.

[36]. Li, C., Liang, B., & Wang, H. (2008). Preparation of synthetic rutile by hydrochloric acid leaching of mechanically activated Panzhihua ilmenite. *Hydrometallurgy,* 91, 121–129.

[37]. Zdujić, M., Jovalekić, C., Karanović, Lj., Mitrić, M., Poleti, D., & Skala, D. (1998). Mechanochemical treatment of α-Fe_2O_3 powder in air atmosphere. *Materials Science and Engineering: A,* 245, 109–117.

نشریه مهندسی معدن و محیط زیست
نشانی نشریه: www.jme.shahroodut.ac.ir
انجمن مهندسی معدن ایران
دانشگاه صنعتی شاهرود

ارزیابی تأثیر فعال‌سازی مکانیکی بر ویژگی‌های ریزساختاری هماتیت با استفاده از پارامتر شکل

بهزاد نعمتی اخگر*

گروه مهندسی معدن، دانشکده فنی و مهندسی، دانشگاه ارومیه، ارومیه، ایران

اطلاعات مقاله

تاریخ ارسال: ۲۰۲۵/۰۶/۱۵
تاریخ داوری: ۲۰۲۵/۰۸/۰۵
تاریخ پذیرش: ۲۰۲۵/۰۹/۲۰

DOI: 10.22044/jme.2025.16522.3231

کلمات کلیدی

هماتیت
XRD
پارامتر شکل
انحلال در اسید سولفوریک
ریزساختار

چکیده

پژوهشگران حوزه‌های مختلف مهندسی به‌طور فزآینده‌ای به بررسی تأثیر ویژگی‌های ریزساختاری کانی‌ها، از جمله هماتیت، بر روی واکنش‌پذیری آنها علاقه‌مند شده‌اند. در این مطالعه رفتار هماتیت و تغییرات ریزساختاری آن در طی فعال‌سازی مکانیکی با استفاده از پارامتر شکل مورد مطالعه قرار گرفت. نتایج حاصل از آنالیز پراش لیزری ثابت نمود پدیده‌ی تجمع ذرات پس از ۶۰ دقیقه فعال‌سازی مکانیکی در هماتیت رخ می‌دهد. بر اساس مطالعات ریزساختاری، میزان بلورینگی هماتیت پس از ۲۴۰ دقیقه فعال‌سازی مکانیکی به کمتر از ۱۶٪ کاهش یافت. همچنین کرنش شبکه ای و اندازه کریستالیت ها در طول فرآیند فعال‌سازی مکانیکی به‌طور پیوسته تغییر کردند که این امر موجب افزایش کارایی انحلال پذیری هماتیت در اسید سولفوریک گردید. نتایج نشان دادند که نرخ تغییر کرنش شبکه ای از سایر پارامترهای ریزساختاری بالاتر است. بر اساس یافته، پارامتر شکل از مقدار اولیه حدود ۰/۳۱ در هماتیت خام پس از ۶۰ و ۲۴۰ دقیقه فعال‌سازی مکانیکی به ترتیب به ۰/۸۸ و ۰/۶۶ در نمونه‌های هماتیت افزایش یافت. بررسی پارامتر شکل آشکار ساخت که پس از ۲۴۰ دقیقه فعال‌سازی مکانیکی، بیشترین بخش انرژی مکانیکی در شبکه هماتیت به صورت کرنش شبکه ای ذخیره می‌شود. با توجه به اثر کمتر کرنش شبکه ای در ارتقاء واکنش‌پذیری هماتیت، می‌توان نتیجه گرفت که زمان‌های کوتاه‌تر فعال‌سازی مکانیکی نسبت به زمان‌های طولانی ترجیح داده می‌شوند؛ زیرا این امر علاوه بر افزایش ظرفیت، موجب کاهش هزینه نیز خواهند شد.

نویسنده مسئول مکاتبات: b.n.akhgar@azad.ac.ir (بهزاد نعمتی اخگر)